Scaling in the Fan of an Unconventional Quantum Critical Point

Roger G. Melko[1,2] and Ribhu K. Kaul[3]

[1]*Department of Physics and Astronomy, University of Waterloo, Ontario, N2L 3G1, Canada*
[2]*Materials Science and Technology Division, Oak Ridge National Laboratory, Oak Ridge Tennessee, 37831, USA*
[3]*Department of Physics, Harvard University, Cambridge Massachusetts, 02138, USA*

(Received 23 July 2007; revised manuscript received 8 October 2007; published 8 January 2008)

We present results of extensive finite-temperature quantum Monte Carlo simulations on a SU(2) symmetric $S = 1/2$ quantum antiferromagnet with four-spin interaction [A. W. Sandvik, Phys. Rev. Lett. **98**, 227202 (2007)]. Our simulations, which are free of the sign problem and carried out on lattices containing in excess of 1.6×10^4 spins, indicate that the four-spin interaction destroys the Néel order at an unconventional $z = 1$ quantum critical point, producing a valence-bond solid paramagnet. Our results are consistent with the ''deconfined quantum criticality'' scenario.

DOI: 10.1103/PhysRevLett.100.017203 PACS numbers: 75.40.Mg, 75.40.Cx

Research into the possible ground states of SU(2) symmetric quantum antiferromagnets has thrived over the past two decades, motivated to a large extent by the undoped parent compounds of the cuprate superconductors. In these materials, the Cu sites can be well described as $S = 1/2$ spins on a two-dimensional (2D) square lattice that interact with an antiferromagnetic exchange, the archetypal model for which is the Heisenberg model. By now, it is well established [1] that the ground state of this model with nearest-neighbor interaction has Néel order that spontaneously breaks the SU(2) symmetry. Two logical questions immediately arise: What possible paramagnetic ground states can be reached by tuning competing interactions that destroy the Néel state? Are there universal quantum critical points (QCP) that separate these paramagnets from the Néel phase?

An answer to the first question is to disorder the Néel state by the proliferation of topological defects in the Néel order parameter [2]. It was shown by Read and Sachdev [3] that the condensation of these defects in the presence of quantum Berry phases results in a fourfold degenerate paramagnetic ground state, which breaks square-lattice symmetry due to the formation of a crystal of valence bonds—a valence-bond solid (VBS) phase. An answer to the second question was posed in recent work by Senthil *et al.* [4], where the possibility of a direct continuous Néel-to-VBS transition was proposed. The natural field-theoretic description of this ''deconfined quantum critical point'' is written in terms of certain fractionalized fields that are confined on either side of the QCP and become ''deconfined'' precisely at the critical point. As is familiar from the general study of QCPs, these fractional excitations are expected to influence the physics in a large fan-shaped region that extends above the critical point at finite-T [5] (see Fig. 1).

It is clearly of great interest to find models that harbor a direct Néel-VBS QCP and that can be studied without approximation on large lattices. Currently, the best candidate is the ''JQ'' model, introduced by Sandvik [6], which is an $S = 1/2$, SU(2) invariant antiferromagnet with an additional four-spin interaction,

$$H_{\rm JQ} = J\sum_{\langle ij\rangle}\mathbf{S}_i\cdot\mathbf{S}_j - Q\sum_{\langle ijkl\rangle}\left(\mathbf{S}_i\cdot\mathbf{S}_j - \frac{1}{4}\right)\left(\mathbf{S}_k\cdot\mathbf{S}_l - \frac{1}{4}\right), \quad (1)$$

where indices are arranged as in the inset of Fig. 1. Using a $T = 0$ projector quantum Monte Carlo (QMC) method on lattices sizes up to 32×32 [6], Sandvik showed that the four-spin interaction destroys Néel order and produces a VBS phase at $J/Q \sim 0.04$. Close to this critical value of J/Q, scaling in the spin and dimer correlation functions suggests a continuous transition with anomalous dimensions of the Néel and VBS order parameters equal, with a common value $\eta = 0.26(3)$. In this Letter, we explore the

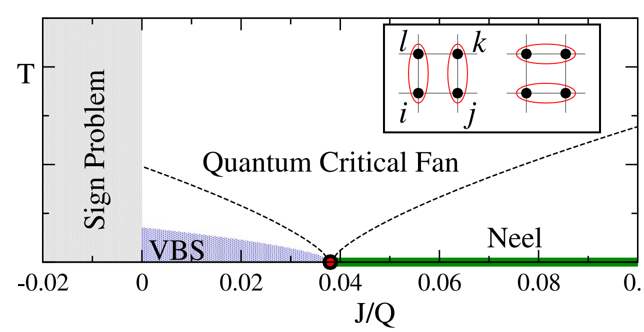

FIG. 1 (color online). Schematic of the proposed T-J/Q phase diagram of the JQ model. Large-scale finite-T simulations presented here substantiate the following: (i) The $T = 0$ Néel order present for $J/Q \gg 1$ is destroyed at a QCP ($J/Q \approx 0.038$); (ii) in the ''quantum critical fan'' there is scaling behavior characteristic of a $z = 1$ QCP, (iii) an accurate estimate of the scaling dimension of the Néel field establishes that this transition is not in the O(3) universality class, and, (iv) the paramagnetic ground state for sufficiently small J/Q is a VBS. In the QMC basis used here, the region with $Q < 0$ is sign problematic. The inset shows how the Q term is written in terms of bonds on a plaquette.

candidate Néel-VBS QCP in the full T-J/Q phase diagram on large lattices using a complementary finite-T QMC technique, the stochastic series expansion (SSE) method with directed loops [7]. The SSE QMC allows access to the physically important quantum critical fan (see Fig. 1), and admits high-accuracy estimates for the spin stiffness ρ_S and the uniform susceptibility χ_u. The scaling of these observables provides strong evidence for a continuous $z = 1$ transition in the JQ model.

Basis and sign of matrix elements.—*A priori*, it is unclear that SSE simulations of $H_{\rm JQ}$ are free of the notorious sign problem: a fluctuating sign in the weights used in the QMC sampling. In the SSE, finding an orthogonal basis in which all off-diagonal matrix elements of the Hamiltonian are nonpositive solves the sign problem. A simple unitary transformation on the S^z basis (a π rotation about the z axis on one sublattice) results in a new basis in which, for $J, Q > 0$, all off-diagonal matrix elements of $H_{\rm JQ}$ are nonpositive, allowing sign-problem free simulations (Fig. 1). We note that this nonpositivity condition is also the main ingredient in the proof of the Marshall sign theorem, allowing us to infer that the ground state of $H_{\rm JQ}$ for $J, Q > 0$ must be a spin singlet. As shown below, this singlet state changes from Néel at $Q \ll J$ to VBS at $J \ll Q$.

Numerical results.—Using the SSE QMC, we studied various physical observables in the JQ model on finite-size lattices of linear dimension L (with number of spins $N_{\rm spin} = L^2$). Particular attention was paid to the scaling of the spin stiffness $\rho_s = \partial^2 E_0/\partial\phi^2$ (E_0 is the energy and ϕ is a twist in the boundary conditions) and the uniform spin susceptibility $\chi_u = \langle(\sum_i S_i^z)^2\rangle/TN_{\rm spin}$. In the S^z basis used here, it is easy to measure the correlation functions $C_N^z(\mathbf{r},\tau) = \langle S^z(\mathbf{r},\tau)S^z(0,0)\rangle$ and $C_V^z(\mathbf{r},\tau) = \langle[S^z(\mathbf{r},\tau)S^z(\mathbf{r}+\hat{\mathbf{x}},\tau)][S^z(0,0)S^z(\hat{\mathbf{x}},0)]\rangle$. While C_N^z is the correlation function of the Néel order parameter, the VBS order is indicated by C_V^z, which is the correlation function of the composite operator $S^z(\mathbf{r})S^z(\mathbf{r}+\hat{\mathbf{x}})$, receiving contribution from both the standard VBS order parameter $\mathbf{S}(\mathbf{r})\cdot\mathbf{S}(\mathbf{r}+\hat{\mathbf{x}})$ as well as the traceless symmetric tensor constructed from $S^i(\mathbf{r})S^j(\mathbf{r}+\hat{\mathbf{x}})$. Structure factors for the Néel and VBS phases are constructed from these correlation functions by Fourier transformation at equal time, $S_{N,V}[\mathbf{q}] = \sum_{\mathbf{r}}[\exp(-i\mathbf{q}\cdot\mathbf{r})C_{N,V}^z(\mathbf{r},\tau=0)]/N_{\rm spin}$, from which the order parameters are defined at the observed ordering wave vectors: $m_{N,V}^2 = S_{N,V}[\mathbf{q}_{N,V}]/N_{\rm spin}$. Zero-frequency susceptibilities (χ_N and χ_V) are constructed by integrating over all τ and Fourier transforming in space to the ordering vectors $\mathbf{q}_{N,V}$.

Examination of the full $\mathbf{q}$-dependent structure factors indicates the presence of sharp ordering wave vectors in S_N [$\mathbf{q}_N = (\pi,\pi)$] for large J/Q and S_V [$\mathbf{q}_V = (\pi,0)$ or $(0,\pi)$] (the latter in the case where the correlator is measured with $\hat{\mathbf{y}}$) for large Q/J [8], confirming the Néel and VBS phases observed in Ref. [6]. As shown in Fig. 2, $T\to 0$ converged data scales convincingly to a nonzero value for m_N^2 at $J/Q = 0.1$ and for m_V^2 at $J/Q = 0.01$. The critical coupling appears to occur between $J_c \approx 0.038$ and 0.040 (we set $Q = 1$ fixed throughout), such that as J_c is approached from above (below) the extrapolated Néel (VBS) order parameter is suppressed. Very near J_c, both order parameters vanish within our error bars, while a power law with no y intercept fits the Néel data with high accuracy. More specifically, at J_c, scaling arguments require $S_N \propto L^{1-\eta_N}\mathbb{X}_S(L^zT/c)$ and $\chi_N \propto L^{2-\eta_N}\mathbb{X}_\chi(L^zT/c)$, with η_N the anomalous dimension of the Néel field. In Fig. 3, we verify this scaling behavior and determine the universal functions $\mathbb{X}_S$ and $\mathbb{X}_\chi$. Both analyses illustrated in Figs. 2 and 3 give a consistent estimate of $\eta_N \approx 0.35(3)$. This

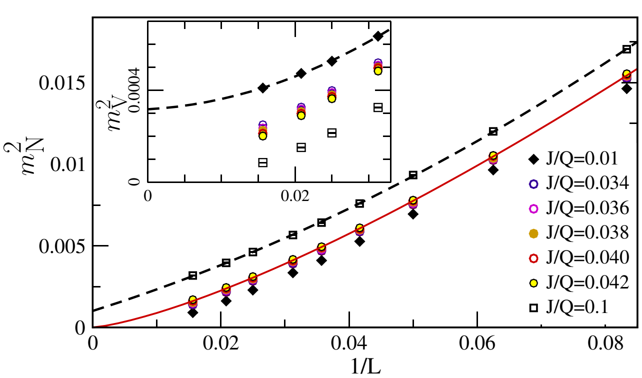

FIG. 2 (color online). $T\to 0$ converged Néel (main) and VBS (inset) order parameters as a function of $1/L$. Dashed lines are quadratic fits that illustrate the finite condensate in the ordered phases. The solid (red) line is a fit to the form $y = c_1x^{c_2}$ (illustrated for $J/Q = 0.040$), where $c_2 = z + \eta_N$ is expected at the critical coupling. In fitting to the nine L values for each J/Q, we find a minimum in the χ^2 value (per degree of freedom) of 3.1 for $J/Q = 0.040$, with $c_2 \approx 1.35(1)$. For $J/Q = 0.038$, the χ^2 value is 3.9, with $c_2 \approx 1.37(1)$. All other J/Q produce much larger χ^2 (greater than 10).

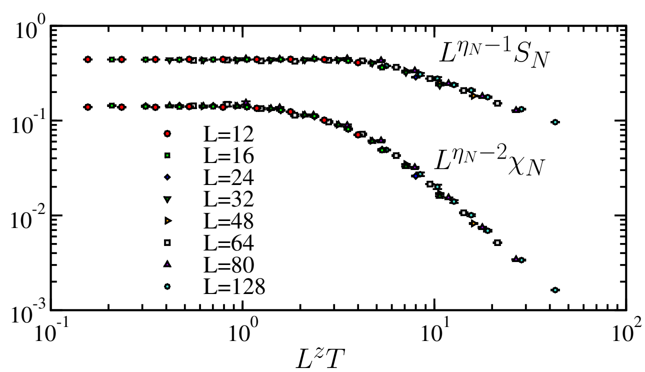

FIG. 3 (color online). Criticality of the Néel field at $J = 0.038$: collapse of the Néel structure factor (S_N) and susceptibility (χ_N) with $z = 1$ and $\eta_N = 0.35$, determining the universal functions $\mathbb{X}_S(x)$ and $\mathbb{X}_\chi(x)$ (up to nonuniversal scale factors on the x and y axes). The only fit parameter for both S_N and χ_N is η_N, the anomalous dimension of the Néel field.

value is larger than the result of $\eta_N \approx 0.26(3)$ from Ref. [6]. While the exact source of this discrepancy is unclear due to the entirely different methods used to extract the exponents, we note that (i) our analysis does not involve extra fit parameters from the inclusion of subleading corrections and (ii) the collapse of both S_N and χ_N takes place over two and a half orders of magnitude of LT with only one common fit parameter, η_N; both facts give us confidence in our estimate. The critical scaling of C_V^z is more complicated; due to the aforementioned mixing in of two order parameters, C_V^z is expected to receive two *independent* power-law contributions. Indeed, it is difficult to disentangle these individual contributions on the limited range of lattice sizes available, precluding us from verifying the proposal [6] that $\eta_N = \eta_V$.

We now turn to an analysis of the scaling properties of χ_u and ρ_s in the hypothesized quantum critical fan region of Fig. 1. χ_u and ρ_s, being susceptibilities of conserved quantities, have no anomalous scaling dimension, and hence at finite T and L in the proximity of a scale-invariant critical point, assuming hyper-scaling,

$$\rho_s(T, L, J) = \frac{T}{L^{d-2}} \mathbb{Y}\left(\frac{L^z T}{c}, gL^{1/\nu}\right), \tag{2}$$

$$\chi_u(T, L, J) = \frac{1}{TL^d} \mathbb{Z}\left(\frac{L^z T}{c}, gL^{1/\nu}\right), \tag{3}$$

where $g \propto (J - J_c)/J_c$. At criticality ($g = 0$), it is easy to see that $\mathbb{Y}(x \to 0, 0) = \mathcal{A}_\rho/x$ and $\mathbb{Z}(x \to \infty, 0) = \mathcal{A}_\chi x^{d/z}$, where $\mathbb{Y}(x, y)$ and $\mathbb{Z}(x, y)$ are universal scaling functions and $\mathcal{A}_\chi$, $\mathcal{A}_\rho$ are universal amplitudes of the quantum critical point, and c is a nonuniversal velocity.

At criticality and $L \to \infty$, one can show from Eq. (3) that $\chi_u = (\mathcal{A}_\chi/c^{d/z})T^{d/z-1}$; i.e., for a $z = 1$ transition, χ_u should be T linear and have a zero intercept on the y axis at $T = 0$ [10]. In Fig. 4, χ_u data for an $L = 128$ system is presented. Within our error bars, this data is $L \to \infty$ converged for the region of T shown; at smaller T the finite-size gap causes an exponential reduction in χ_u. The inset shows how the extracted value of the y intercept, a (from a fit to the form $a + bT$), changes sign as the coupling is tuned, consistent with $0.036 \leq J_c \leq 0.040$ and demonstrating to high precision the $z = 1$ scaling.

Turning to study Eqs. (2) and (3) further, one may hold the first argument of the universal functions fixed by setting $L = 1/T$ (assuming $z = 1$ as indicated above). In order to achieve this, we performed extensive simulations on lattice sizes up to $L = 1/T = 64$, illustrated in Fig. 5. According to Eqs. (2) and (3), data curves for $L\rho_s$ and $L\chi_u$ plotted versus J should show a crossing point with different L precisely at J_c. We find that for relatively large sizes ($32 \leq L \leq 64$) the crossing point converges quickly in the interval $0.038 \leq J \leq 0.040$. The insets show the data collapse when the x axis is rescaled to $gL^{1/\nu}$ (with $\nu = 0.68$). We note that with the inclusion of small subleading corrections

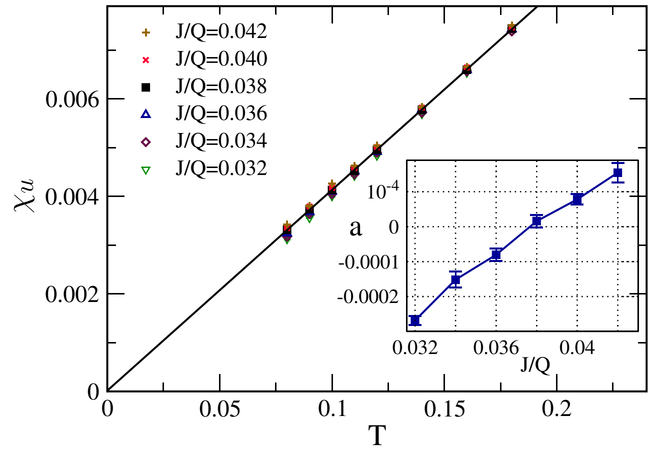

FIG. 4 (color online). Finite-T uniform susceptibility, for a $L = 128$ system near J_c. Error bars are much smaller than the symbol size. For the region $0.08 \leq T \leq 0.18$, the data is highly linear, and a straight-line fit for $J/Q = 0.038$ (shown) intercepts the origin within error bars. Intercepts of straight-line fits for all data sets are in the inset. From the slope of the linear-T behavior we obtain $\mathcal{A}_\chi/c^2 = 0.0412(2)$.

(of the form a_ω/L^ω), the crossing point and data collapse of ρ_s and χ_u can be made consistent, at the expense of two more fit parameters, even for much smaller system sizes than illustrated [9]. In contrast to the U(1) symmetric JK model [11], where the absence of a T-linear χ_u and a crossing in the data for $\rho_s L$ cast doubt on its interpretation as a $z = 1$ QCP, the present data for this SU(2) symmetric model gives strong support for a $z = 1$ QCP between $0.038 \leq J \leq 0.040$.

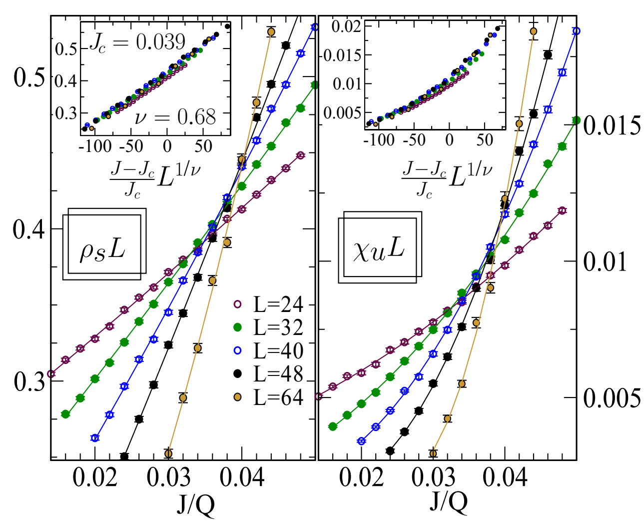

FIG. 5 (color online). Zoom-in of the spin stiffness and susceptibility close to the expected critical point, taken for simulation cells of size $L = 1/T$. Data in the inset is scaled to get the best collapse for the largest system sizes, which occurs for $J_c \sim 0.039(1)$ and $\nu \sim 0.68(4)$.

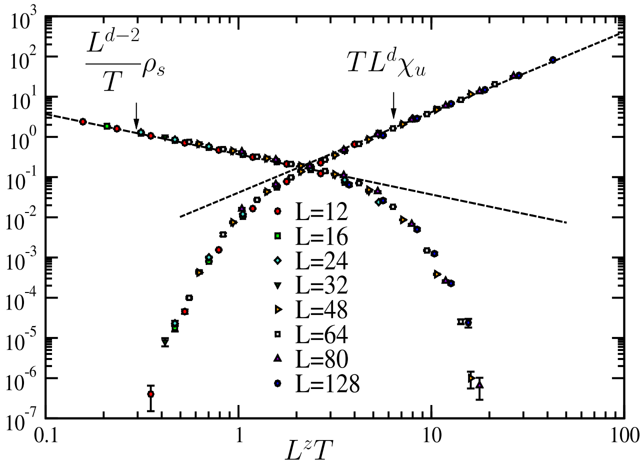

FIG. 6 (color online). Scaling of χ_u and ρ_s at $J = 0.038 \approx J_c$, with $z = 1$ and $d = 2$. These plots are the universal functions $\mathbb{Y}(x, 0)$ and $\mathbb{Z}(x, 0)$ up to the nonuniversal scale factor c on the x axis. The expected asymptotes (see text) are plotted as dashed lines $\mathbb{Y}(x \to 0, 0) = \mathcal{A}_\rho/x$ and $\mathbb{Z}(x \to \infty, 0) = \mathcal{A}_\chi x^{d/z}$. From fits to the data, we find $\mathcal{A}_\chi/c^2 = 0.041(4)$ and $\mathcal{A}_\rho c = 0.37(3)$, allowing us to estimate a universal model-independent number associated with the QCP, $\mathcal{A}_\rho\sqrt{\mathcal{A}_\chi} \approx 0.075(4)$.

Finally, we hold the second argument of the scaling functions [Eqs. (2) and (3)] constant by tuning the system to $g = 0$. One then expects a data collapse for ρ_s/T and $L\chi_u$ when they are plotted as a function of L^zT (with $z = 1$). Figure 6 shows this collapse for simulations carried out with extremely anisotropic arguments LT, varying over almost 3 orders of magnitude. There is an excellent data collapse over 8 orders of magnitude of the range of the universal functions, with no fit parameters. This data together with that in Fig. 4 provide our most striking evidence for the existence of a QCP with $z = 1$ in the proximity of $J/Q \approx 0.038$.

Discussion.—In this Letter we have presented extensive data for the SU(2) symmetric JQ model which indicates that the Néel order (present when $J \gg Q$) is destroyed at a continuous quantum transition as Q is increased [6]. In the finite-T quantum critical fan above this QCP, scaling behavior is found that confirms the dynamic scaling exponent $z = 1$ to high accuracy. The anomalous dimension of the Néel field at this transition is determined to be $\eta_N \approx 0.35(3)$, almost an order of magnitude more than its value of 0.038 [12] for a conventional O(3) transition. For sufficiently large values of Q we find that the system enters a spin-gapped phase with VBS order. To the accuracy of our simulations, our results are fully consistent with a direct continuous QCP between the Néel and VBS phases, with a critical coupling between $J/Q \approx 0.038$ and $J/Q \approx 0.040$. Although our finite-size study cannot categorically rule out a weak first-order transition, we have found no evidence for double-peaked distributions, indicating an absence of this sort of first-order behavior on the relatively large length scales studied here. It is interesting to compare our results to the only theory currently available for a continuous Néel-VBS transition: the deconfined quantum criticality scenario [4], in which the Néel-VBS transition is described by the noncompact $\mathbb{CP}^1$ field theory. All of the qualitative observations above, including an unusually large η_N [13], agree with the predictions of this theory. Indeed, our estimate of $\eta_N \approx 0.35$ [Fig. 3] is in remarkable numerical agreement with a recent field-theoretic computation [14] of this quantity, which finds $\eta_N = 0.3381$. With regard to other detailed quantitative comparisons, we have provided the first step by computing many universal quantities, $\mathbb{X}_\chi(x)$, $\mathbb{X}_S(x)$, $\mathbb{Y}(x, 0)$, $\mathbb{Z}(x, 0)$, and $\mathcal{A}_\rho\sqrt{\mathcal{A}_\chi} \approx 0.075$ [Fig. 6] in the JQ model. Analogous computations in the $\mathbb{CP}^1$ model, although currently unavailable [15], are highly desirable to further demonstrate that the JQ model realizes this new and exotic class of quantum criticality.

We acknowledge scintillating discussions with S. Chandrasekharan, A. del Maestro, T. Senthil, and especially S. Sachdev and A. Sandvik. This research (R. G. M.) was sponsored by DOE Contract No. DE-AC05-00OR22725. R. K. K. acknowledges financial support from NSF DMR-0132874, DMR-0541988, and DMR-0537077. Computing resources were contributed by NERSC (DOE Contract No. DE-AC02-05CH11231), NCCS, the HYDRA cluster at Waterloo, and the DEAS and NNIN clusters at Harvard.

[1] E. Manousakis, Rev. Mod. Phys. **63**, 1 (1991).
[2] F. D. M. Haldane, Phys. Rev. Lett. **61**, 1029 (1988).
[3] N. Read and S. Sachdev, Phys. Rev. B **42**, 4568 (1990).
[4] T. Senthil *et al.*, Science **303**, 1490 (2004); Phys. Rev. B **70**, 144407 (2004).
[5] S. Sachdev, *Quantum Phase Transitions* (Cambridge University Press, New York, 1999).
[6] A. W. Sandvik, Phys. Rev. Lett. **98**, 227202 (2007).
[7] O. F. Syljuåsen and A. W. Sandvik, Phys. Rev. E **66**, 046701 (2002); R. G. Melko and A. W. Sandvik, Phys. Rev. E **72**, 026702 (2005).
[8] The VBS order is also visible in measurements of correlation functions between off-diagonal terms [9].
[9] R. K. Kaul and R. G. Melko (unpublished).
[10] A. V. Chubukov *et al.*, Phys. Rev. B **49**, 11 919 (1994).
[11] A. W. Sandvik and R. G. Melko, arXiv:cond-mat/0604451; Ann. Phys. (N.Y.) **321**, 1651 (2006).
[12] M. Campostrini *et al.*, Phys. Rev. B **65**, 144520 (2002).
[13] O. I. Motrunich and A. Vishwanath, Phys. Rev. B **70**, 075104 (2004).
[14] Z. Nazario and D. I. Santiago, Nucl. Phys. **B761**, 109 (2007).
[15] A. Kuklov *et al.*, Ann. Phys. (N.Y.) **321**, 1602 (2006) found a discontinuous transition in a U(1) deformation of the $\mathbb{CP}^1$ model. Results relevant to the SU(2) invariant H_{JQ} are so far unavailable (see, however, [13]).